



ANNUAL
REVIEWS **Further**

Click [here](#) for quick links to Annual Reviews content online, including:

- Other articles in this volume
- Top cited articles
- Top downloaded articles
- Our comprehensive search

Keynote Topic

This article is part of the **Oxide Electronics** keynote topic compilation.

Correlated Oxide Physics and Electronics

J.H. Ngai,¹ F.J. Walker,^{2,3} and C.H. Ahn^{2,3,4}

¹Department of Physics, University of Texas, Arlington, Texas 76019

²Center for Research on Interface Structures and Phenomena, ³Department of Applied Physics, and ⁴Department of Mechanical Engineering and Materials Science, Yale University, New Haven, Connecticut 06520; email: charles.ahn@yale.edu

Annu. Rev. Mater. Res. 2014. 44:1–17

The *Annual Review of Materials Research* is online at matsci.annualreviews.org

This article's doi:
10.1146/annurev-matsci-070813-113248

Copyright © 2014 by Annual Reviews.
All rights reserved

Keywords

transition metal oxides, correlated phenomena, superconductivity, magnetism, metal-insulator transitions

Abstract

Transition metal oxides exhibit a range of correlated phenomena with applications to novel electronic devices that possess remarkable functionalities. This article reviews recent progress in elucidating both mechanisms that govern correlated behavior in transition metal oxides and advancements in device fabrication that have enabled strong correlations to be controlled through applied electric fields. Advancements in the growth of transition-metal-oxide films and artificial heterostructures have enabled superconductivity, magnetism, and metal-insulator transitions to be controlled in cuprates, manganites, and vanadates by using the electric field effect. In addition, interfaces between transition metal oxides have recently emerged as a setting in which strong correlations can be manipulated in two dimensions to realize unusual quantum-ordered phases. Finally, key relationships between structure and transport in ultrathin films of transition metal oxides have been elucidated. Coupling the structural degrees of freedom in oxides to applied electric fields thus opens new pathways to control correlated behavior in devices.

INTRODUCTION

Transition metal oxides (TMOs) are characterized by strong correlations that give rise to a variety of electronic phases, including ferromagnetism, superconductivity, and other charge- and spin-ordered states. Such phenomena arise from the complex interplay between the charge, spin, orbital, and lattice degrees of freedom that are inherent in many TMOs, as illustrated in **Figure 1**. Two of the best-known examples of correlated TMOs are the cuprates and manganites; the former exhibits high-temperature superconductivity and the latter colossal magnetoresistance (CMR). The formation of correlated phases remains one of the greatest challenges to our understanding of emergent phenomena in condensed matter systems. Thus, the study of correlated behavior in TMOs is of fundamental importance.

Beyond fundamental interest, correlated behavior in TMOs also provides a pathway to realize novel electronic devices in which magnetism, superconductivity, and metal-insulator transitions can be controlled by using an externally applied electric field or signal. The basic premise behind correlated devices is illustrated in the generic phase diagram shown in **Figure 2a**. Phases A and B represent two phases with dissimilar electronic characteristics. The approach is to actively and reversibly induce a change in the phase of the TMO as a means to modulate device behavior (1). For example, if phases A and B represent insulating and metallic phases, then switching the TMO between the two phases can form the basis for memory or logic applications. Similarly, magnetic phases exhibited by TMOs can lead to novel devices in which applied electric fields can control magnetism. Such novel functionalities cannot be achieved by using conventional semiconductors alone.

Recent advancements in thin-film growth have allowed correlated phases for electronic devices to be exploited. TMO thin films can be synthesized with atomic-scale precision by using advanced techniques such as molecular beam epitaxy (shown in **Figure 2b**). Such control of growth allows oxides differing in chemical composition to be epitaxially combined in layered heterostructures, in which atomic-scale structure, carrier density, and dimensionality can be manipulated. The control

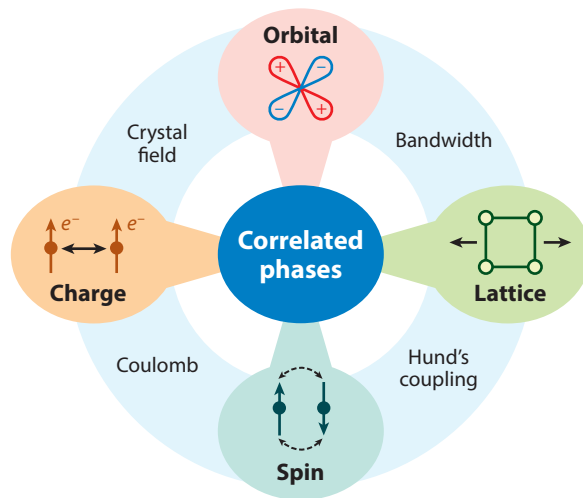


Figure 1

Electronic and structural degrees of freedom. The interplay between charge, orbital, lattice, and spin degrees of freedom gives rise to correlated phases in transition metal oxides.

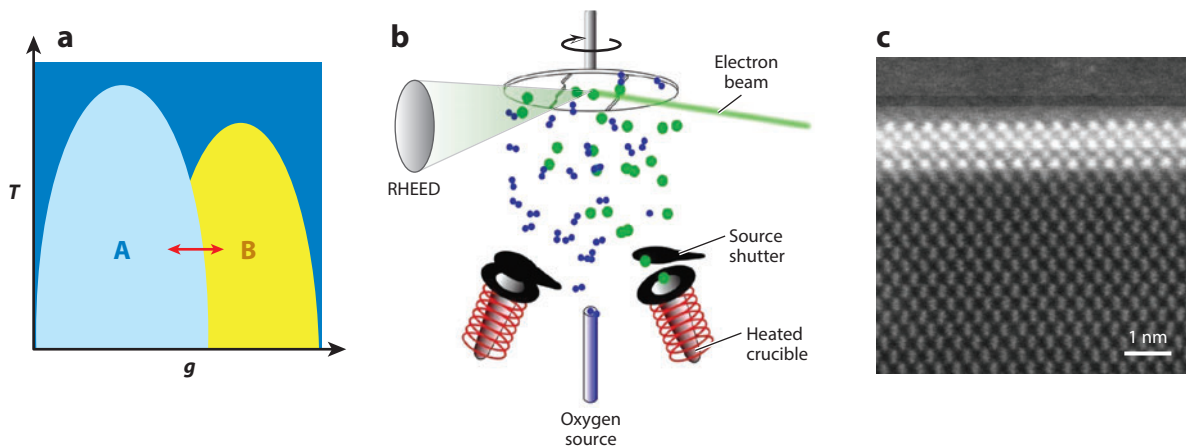


Figure 2

Thin films and phase control. (a) Generic phase diagram. Active switching of material between phases A and B (red arrow) through an applied electric field forms the basis for correlated oxide electronics. Abbreviations: T , temperature; g , generic variable (e.g., bandwidth, doping) that enables the oxide to transition from one phase to another. (b) Advanced thin-film-growth techniques such as molecular beam epitaxy enable transition metal oxides (TMOs) to be integrated into artificial heterostructures. Reflection high-energy electron diffraction (RHEED) enables in situ characterization of epitaxial heterostructures that form the basis for correlated oxide devices. Panels *a* and *b* reproduced from Reference 31. (c) Two-and-a-half unit cells of SrTiO_3 grown on Si (100). Molecular beam epitaxy enables TMOs to be epitaxially integrated with established technology platforms. Reproduced from Reference 3.

of such parameters is essential for manipulating correlated behavior in TMOs. Furthermore, the epitaxial growth of a TMO directly on Si allows such heterostructures to be integrated with established technology platforms, as shown in **Figure 2c** (2, 3).

Advancements in the growth of TMO thin films and heterostructures have come at a time when the performance of the complementary metal oxide semiconductor (CMOS) transistors ubiquitously found in all electronic devices has reached a plateau. This plateau in performance is due in part to the fundamental materials constraints of Si. Limitations in carrier mobility and fluctuations in carrier density can contribute to short-channel effects, which become more pronounced as transistors are scaled to smaller dimensions. Recognizing the potential that TMOs could play in the development of post-CMOS electronics, the International Technology Roadmap for Semiconductors categorized TMOs as emerging research materials (4). At present, electronic devices based on correlated TMOs are years away from commercialization. However, key progress in materials growth and device fabrication has opened new pathways to control correlated phenomena through applied electric fields. Field-effect transistors in which magnetism, superconductivity, and metal-insulator transitions can be controlled have become a reality. With regard to materials development, interfaces between electrically dissimilar oxides have recently emerged as a setting in which strong correlations can be manipulated to realize coexisting quantum states of matter. Finally, key relationships between structure and transport in ultrathin films of correlated TMOs have been elucidated. Such relationships can potentially enable correlated behavior to be controlled by modifying atomic-scale structure with applied electric fields. This article aims to review these key developments and to outline future directions to be taken in the development of correlated TMO devices. This article is not intended to be a comprehensive review, as emphasis is given to some of the work of the authors.

TUNING CORRELATED BEHAVIOR IN TRANSITION METAL OXIDES

In essence, correlated phenomena in TMOs derive from the competition between (a) kinetic hopping of carriers and (b) localization due to Coulomb repulsion between carriers. These strong interactions are not adequately accounted for in conventional band structure models, nor can their effects be fully captured by enhancing the effective mass of carriers, as used in Fermi liquid theory. The strong interactions can lead to the opening of a gap in the partially filled d -bands of TMOs, resulting in the creation of upper and lower Hubbard bands. For this class of oxides, a TMO is classified as a charge-transfer (or a Mott-Hubbard) insulator if the energy of the oxygen $2p$ band is situated above (or below) the lower Hubbard band (5). For both types of insulators, correlated phases emerge as the competition between localization and carrier itinerancy is tuned. For example, localization and itinerancy in Mott-Hubbard insulators are typically described by the parameters U and W , where the former describes on-site Coulomb repulsion and the latter is the single-particle bandwidth. In the limit in which $U/W > 1$ (< 1), insulating (metallic) behavior is generally exhibited. In the intermediate regime of $U/W \sim 1$, the competition between localization and itinerancy can give rise to a range of correlated phases, depending on the specific electronic and structural properties of the TMO (6). How such states emerge from the competition between localization and kinetic hopping continues to be a topic of active theoretical investigation.

In actual materials, tuning the competition between localization and kinetic hopping involves modulating carrier density or introducing structural changes that affect bandwidth (6). The former approach is known as filling control, whereas the latter is known as bandwidth control. For bulk materials, filling and bandwidth control are typically achieved through chemical substitution. For example, in the $ReNiO_3$ system (where Re denotes rare earth), the bandwidth can be reduced (enhanced) by substituting rare-earth ions of decreasing (increasing) size. Filling control is enabled through the substitution of nonisovalent cations to introduce changes to the carrier density. For example, hole-like carriers are introduced into $La_{1-x}Sr_xMnO_3$ by substituting trivalent rare-earth La with divalent alkaline-earth Sr. Although effective in bulk materials, chemical substitution is not suitable for tuning correlations in devices, in which active control through applied electric fields is desired.

In this regard, the integration of TMOs into artificial heterostructures has allowed carrier density to be controlled through field-effect gate doping (7). The basic device geometry of a semiconductor field-effect transistor can also be utilized to gate dope TMO materials. As shown in **Figure 3**, an electric field is applied through an insulating dielectric to attract or repel carriers from a conducting channel made of a correlated TMO. Unlike chemical substitution, electrostatic doping is a form of filling control that does not introduce additional disorder into materials. Carriers are accumulated or depleted from a region that has a characteristic thickness determined

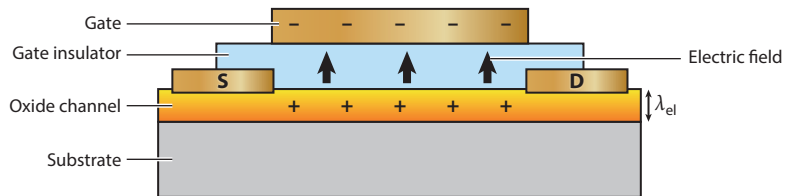


Figure 3

Electrostatic control of correlated phases in transition metal oxides (TMOs). Geometry of electric-field-effect devices for electrostatically doping TMO-based channel materials. For effective modulation of carrier density, the thickness of the TMO channel should be comparable to the electrostatic screening length λ_{el} . D and S denote drain and source, respectively.

by the electrostatic screening length λ_{el} . Due to the high carrier densities of correlated TMOs, λ_{el} is limited to a few angstroms (8). The high carrier densities present two critical challenges in the development of TMO-based field-effect devices. First, very high changes to carrier density need to be achieved to alter electronic correlations, and thus gate materials must exhibit high dielectric constants and breakdown fields. Second, the thicknesses of correlated TMO channels in field-effect devices must be comparable to λ_{el} to avoid shunting effects. Significant progress has been made in the growth of TMO thin films and heterostructures to overcome these challenges. The electric field effect has successfully controlled correlated behavior in a variety of TMOs, such as superconductivity in cuprates, magnetism in manganites, and metal-insulator transitions in nickelates and vanadates. We review these experiments below.

In addition, interfaces between polar and nonpolar TMOs have recently emerged as a setting in which strong correlations can be manipulated to produce quantum phases that are confined to two dimensions. The reduced dimensionality and electronic structure found at interfaces can produce correlated effects that are not observed in the bulk of the constituent compounds forming the interface. For example, magnetism has been found at the interface between the two nonmagnetic oxides LaAlO_3 and SrTiO_3 . Correlated behavior found at TMO interfaces can be manipulated by integrating such interfaces into electric-field-effect devices. We also review these developments in the study of interfaces below.

Finally, recent progress has been made in elucidating relationships between electronic transport and atomic-scale structure in ultrathin films of correlated TMOs. Surfaces and interfaces alter the atomic-scale structure in ultrathin films of a TMO, leading to pronounced effects on carrier bandwidth and transport. Such relationships between structure and transport could potentially be exploited to control correlated behavior in devices. Novel device geometries that utilize applied electric fields to alter structure were recently proposed. We also discuss these developments below.

ELECTROSTATIC CONTROL OF MAGNETISM

One of the more alluring aspects of utilizing correlated materials in devices is the possibility of realizing functionalities that cannot be achieved by using conventional semiconductors alone. One such functionality is the ability to control magnetism through applied electric fields. Devices that enable magnetism to be manipulated through applied electric fields would have tremendous use in spintronics and electromagneto-optical applications. Several naturally occurring materials, such as YMnO_3 and BiFeO_3 , exhibit multiferroic behavior in which magnetic and electric order parameters coexist and are coupled through the lattice (9). However, the coupling between magnetic and electric order parameters in such materials is typically weak. In comparison, multiferroic coupling can be enhanced through the design and growth of layered heterostructures composed of magnetic and ferroelectric materials. In such heterostructures, coupling between electric and magnetic orders occurs via proximity effects near interfaces.

Heterostructures composed of the manganite $\text{La}_{1-x}\text{Sr}_x\text{MnO}_3$ ($x = 0.2$) and the ferroelectric $\text{Pb}(\text{Zr}_{0.8}\text{Ti}_{0.2})\text{O}_3$ (PZT) provide an example of magnetoelectric (x) coupling in artificial heterostructures, as shown in **Figure 4**. In such heterostructures, ultrathin (11-unit-cell-thick) films of $\text{La}_{1-x}\text{Sr}_x\text{MnO}_3$ grown on SrTiO_3 substrates are capped with an epitaxial layer of PZT. $\text{La}_{1-x}\text{Sr}_x\text{MnO}_3$ has a rich phase diagram that exhibits ferromagnetic metallic and insulating phases that can be accessed by controlling the carrier density. The composition of the $\text{La}_{1-x}\text{Sr}_x\text{MnO}_3$ ($x = 0.2$) used in the magnetoelectric devices coincides with a phase boundary between insulating and ferromagnetic metallic phases. Switching the ferroelectric polarization of the PZT layer induces changes in the carrier density within λ_{el} of the $\text{La}_{1-x}\text{Sr}_x\text{MnO}_3$ layer below, thus inducing changes in the magnetization. The change in magnetization was determined through transport,

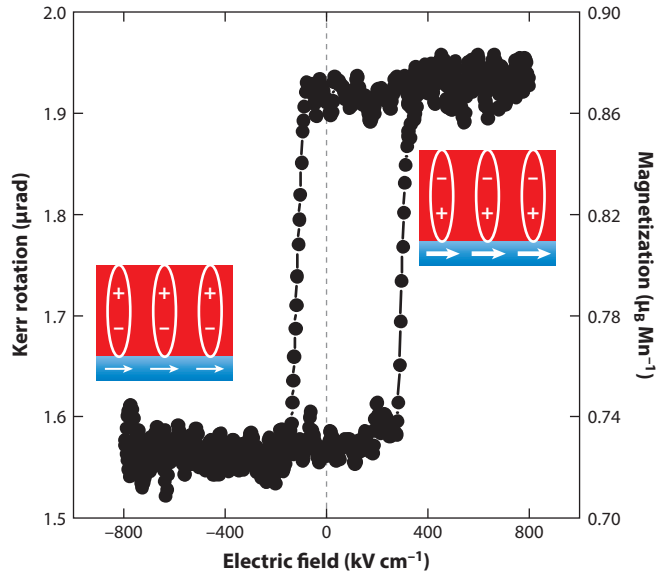


Figure 4

Electric field control of magnetism. The magnetoelectric hysteresis curve shows the magnetic response of a $\text{La}_{1-x}\text{Sr}_x\text{MnO}_3$ channel ($x = 0.2$) and a $\text{Pb}(\text{Zr}_{0.8}\text{Ti}_{0.2})\text{O}_3$ gate as a function of the electric field applied to the gate. The two magnetization values correspond to modulation of the magnetization of the $\text{La}_{1-x}\text{Sr}_x\text{MnO}_3$ channel. The insets represent the magnetic and electric states of the $\text{La}_{1-x}\text{Sr}_x\text{MnO}_3$ and $\text{Pb}(\text{Zr}_{0.8}\text{Ti}_{0.2})\text{O}_3$ layers. The thickness and size of the arrows qualitatively indicate the magnetization amplitude. Reproduced from Reference 10.

magnetic susceptibility, and optical measurements; Kerr rotation of polarized light was utilized in the optical measurements (10). Near-edge X-ray absorption spectroscopy confirms that the magnetoelectric coupling observed in $\text{La}_{1-x}\text{Sr}_x\text{MnO}_3/\text{PZT}$ heterostructures arises from a change in the valence of the Mn ions induced by electrostatic doping through the PZT gate (11).

Besides inducing changes in areal carrier density on the order of $\sim 10^{13}\text{--}10^{14}\text{ cm}^{-2}$, the use of PZT as a gate dielectric also enables nonvolatile control; i.e., the correlated state of the field-effect device is retained after the applied gate voltage is removed. Nonvolatile devices based on TMOs could be exploited in memory and logic applications. For the latter, nonvolatility would provide several advantages over conventional field-effect transistors, namely reduced power consumption, instant-on computing, and dynamic hardware and software coexecution. As the demand for mobile battery-powered electronic devices increases, such features become increasingly desirable.

SUPERCONDUCTIVITY

Some of the earliest work on correlated TMO field-effect devices focused on modulating superconductivity in cuprates. For example, early devices that used SrTiO_3 as the gate material were successful in introducing moderate shifts in the superconducting transition temperature of $\text{YBa}_2\text{Cu}_3\text{O}_{7-\delta}$ (12). The early work on cuprates demonstrated that superconductivity could be controlled through electrostatic doping, provided that the modulation in carrier density was sufficiently large. Later, the introduction of ferroelectric gates, such as PZT, significantly enhanced the changes to carrier density that could be achieved. The larger changes in carrier density enabled underdoped films of $\text{GdBa}_2\text{Cu}_3\text{O}_{7-x}$ to be switched between superconducting behavior and insulating behavior (13).

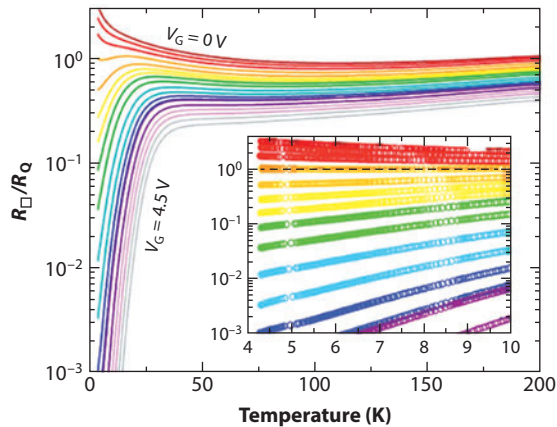


Figure 5

Electric field control of high-temperature superconductivity. Modulation of the superconducting transition temperature in ultrathin films of an underdoped $\text{La}_{2-x}\text{Sr}_x\text{CuO}_4$ channel using an ionic liquid gate. Such experiments revealed that phase fluctuations determine the disappearance of superconductivity in the pseudogap regime. Reproduced with permission from Reference 16.

The need to induce large changes in carrier density in TMO field-effect devices has motivated the search for alternative materials that could replace conventional gate dielectrics. In this regard, large changes in sheet carrier density exceeding $\sim 10^{15} \text{ cm}^{-2}$ were recently achieved by using ionic liquids. In ionic liquid-based field-effect transistors, application of an electric field between a conducting TMO channel and a metallic electrode causes ions to collect near the surface of the TMO, forming a type of capacitor referred to as an electric double layer, in which, unlike the case for conventional dielectric materials, the drop in applied gate voltage occurs over a very short distance near the surface of the TMO channel. Thus, electric fields and changes to sheet carrier density can be exceptionally large. Such ionic liquid gates have been utilized to induce superconductivity both near the surfaces of nominally insulating single-crystal substrates of SrTiO_3 and in ZrNCl films (14, 15).

Recently, a more detailed study of the superconducting-insulator transition in underdoped cuprates was performed by using an ionic liquid gate (16). Using molecular beam epitaxy, Bollinger et al. (16) successfully fabricated unit-cell-thick films of $\text{La}_{2-x}\text{Sr}_x\text{CuO}_4$ at various doping levels. By varying the polarity and magnitude of the gate voltage, hole-type carriers were accumulated and depleted in the cuprate thin films, leading to enhancement and suppression of the superconducting transition temperature and normal-state sheet resistance, respectively, as shown in **Figure 5**. Systematic tuning of the carrier density revealed that the superconductor-insulator transition follows a universal scaling behavior. Beyond enabling electric field control of superconductivity in cuprates, the electric-double-layer transistor also revealed fundamental information on the physics governing pairing in underdoped cuprates. The critical resistance for the superconductor-insulator transition was revealed to be precisely the quantum resistance for Cooper pairs, $h/(2e)^2$, indicating that phase fluctuations, and not pair breaking, determine the disappearance of superconductivity in the underdoped regime (17). Such information is critical to our understanding of the nature of the pseudogap and the microscopic mechanism behind high-temperature superconductivity (18, 19).

The manipulation of superconductivity in devices can also be achieved in a dynamic manner by introducing disequilibrium that suppresses the superconducting order parameter. For example, the

injection of spin-polarized carriers disturbs the equilibrium of the quasiparticle spectrum for the superconductor, namely an imbalance in the densities of spin-up versus spin-down quasiparticles (20). Because pairing in cuprates is singlet in nature, the predominance of one type of spin orientation suppresses the recombination of quasiparticles into pairs. Such spin injection experiments were performed on layered, epitaxial heterostructures composed of cuprates and half-metallic manganites, where the latter was a source of spin-polarized carriers (21–25). Transport measurements showed a suppression of the critical current density in cuprate thin films as a function of injected spin-polarized carriers.

MOTT METAL-INSULATOR TRANSITIONS

Beyond experiments on cuprates, field-effect experiments using ionic electrolyte gates were recently extended to nickelates and vanadates, which are systems that exhibit metal-insulator transitions. Interest in controlling metal-insulator transitions in TMOs stems from the potential of utilizing such materials in memory and logic devices. Scherwitzl et al. (26) modulated the metal-insulator transition temperature in ultrathin films of NdNiO_3 (Figure 6). In the bulk, NdNiO_3 exhibits a first-order transition between a paramagnetic metallic state to an antiferromagnetic insulating state near ~ 200 K. By growing ultrathin films of NdNiO_3 on LaAlO_3 substrates,

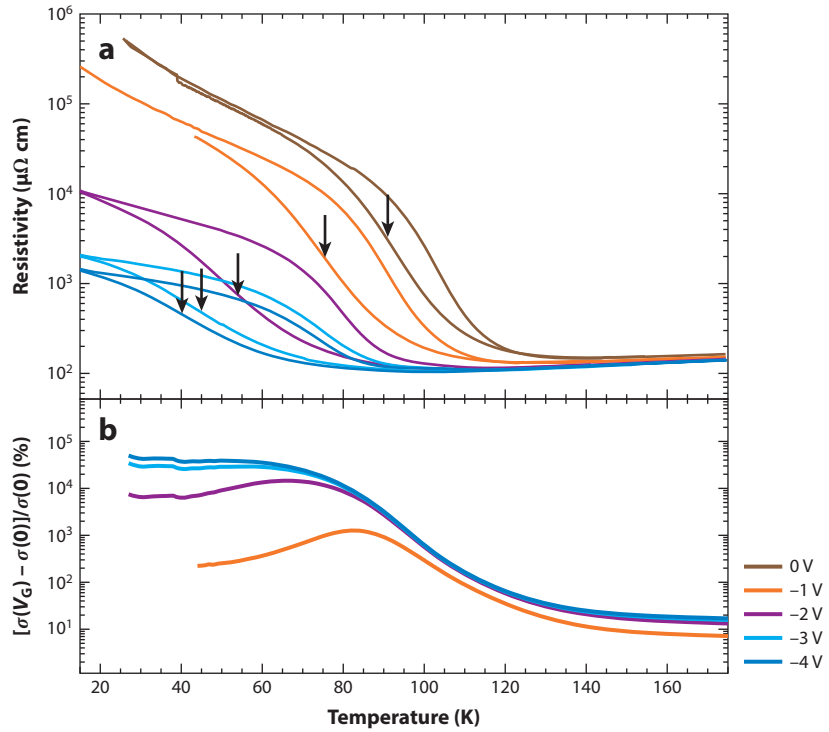


Figure 6

Electric field control of a metal-insulator transition. (a) Modulation of the metal-insulator transition temperature in ultrathin films of NdNiO_3 by using an ionic liquid gate. Arrows represent the nominal transition temperature of the metal-insulator transition. (b) Electroconductivity as a function of temperature and applied gate voltage. Reproduced with permission from Reference 26.

compressive strain was imparted to the films, which reduced the metal-insulator transition to 90 K. By using an ionic liquid gate and thus electrostatically adding hole-type carriers, the transition temperature was subsequently further reduced from 90 to 41 K. Hall measurements indicated that $\sim 3 \times 10^{15} \text{ cm}^{-2}$ or $480 \mu\text{C cm}^{-2}$ charges were added to the NdNiO_3 films, which represents a 21% change in the volume carrier density for the eight-unit-cell-thick films used in Scherwitzl et al.'s study. Similarly, Ha et al. (27) also used ionic liquids to electrostatically dope and induce modest shifts in the metal-insulator transition temperature in the nickelate SmNiO_3 .

Thus far, our discussion on modulating carrier density focuses on gate doping through externally applied electrostatic fields. Carriers can also be electrostatically doped by exploiting internal fields arising at heterojunctions between materials of dissimilar band alignments and electron chemical potentials. For example, Son et al. (28) introduced electron-like carriers into a 2.5-nm-thick layer of NdNiO_3 through an adjacent layer of SrTiO_3 that was doped with La cations. The transfer of charge carriers arises from equilibrating the respective electron chemical potentials of La-doped SrTiO_3 and NdNiO_3 at the interface (28). Son et al. modulated the carrier density by 6% and induced moderate shifts in the metal-insulator transition temperature in NdNiO_3 . Introducing carriers through an adjacent doped oxide layer is analogous to the technique of modulation doping used extensively in compound semiconductor devices.

In the above examples, the manipulation of superconductivity and metal-insulator behavior through field-effect gate doping was achieved in ultrathin films that were limited to a few unit cells in thickness. The short λ_{el} intrinsic to TMOs necessitates the use of ultrathin channels so that appreciable changes in carrier density can be achieved.

In this regard, recent experiments by Nakano et al. (29) on VO_2 are noteworthy in that an electric field applied through an ionic liquid gate modified the conductivity of films that far exceeded λ_{el} in thickness. VO_2 is a Mott insulator that exhibits a metal-insulator transition near 340 K associated with a first-order transition from tetragonal to monoclinic symmetry. Nakano et al. suppressed the sharp metal-insulator transition in films up to 70 nm thick. To explain the unexpected suppression of the metal-insulator transition in thick films, Nakano et al. suggested that carriers electrostatically doped near the surface induced a phase transition that delocalized carriers throughout the film. Inducing phase transitions in films thicker than λ_{el} would represent a significant advancement over previous field-effect experiments and a new paradigm for controlling correlated behavior through electrostatic doping. However, similar field-effect experiments by Jeong et al. (30) indicate that the suppression of the metal-insulator transition in VO_2 can be attributed largely to the creation of oxygen vacancies by the ionic liquid. Thus, electric fields applied through ionic liquid gates appear to induce motion of both electrons and oxygen ions in VO_2 . Further work will be necessary to fully elucidate the effects of ionic liquid gates on VO_2 channels.

The ionic liquid field-effect experiments on VO_2 highlight the challenges associated with finding suitable gate materials that can modulate the high carrier densities in TMOs. Ionic liquid gates, although effective in introducing large changes in carrier density and creating proof-of-concept devices, are not amenable to practical implementation, given the slow switching speeds. Furthermore, lingering questions surrounding the stability of TMOs and the reactivity of TMOs to organic electrolytes have not been fully resolved (27). In comparison, ferroelectric gate materials have been shown to be effective in introducing moderate changes in carrier density. Furthermore, ferroelectric gate materials enable nonvolatile devices to be developed, unlike the case for ionic liquid gates, which require continuous application of a gate voltage. Increasing the polarization of ferroelectric gate materials is necessary to enhance changes in carrier density (31). Thus, a high priority is to develop gate materials that are chemically stable, have low electrical leakage, and form interfaces with TMOs that are free of defect states that trap charge.

CONTROLLING CORRELATED BEHAVIOR AT TRANSITION-METAL-OXIDE INTERFACES

The challenges associated with fabricating TMO channels that are limited in thickness to λ_{el} in field-effect devices highlight the need to create correlated systems in which carriers are naturally confined in two dimensions. Therefore, interfaces between TMOs have recently emerged as a setting in which two-dimensional correlated systems can be realized (32). Interfaces between electronically dissimilar materials are typically characterized by band offsets and discontinuities in polarization and electron chemical potentials. The latter types of discontinuities can be compensated for or equilibrated by transferring charge across the interface from one material to the other. These concepts have been developed in the study of interfaces between conventional semiconductors and have led to the realization of many useful devices, including high-mobility transistors and semiconducting lasers (33, 34). Such concepts of charge transfer naturally carry over to the study of oxide interfaces.

However, unlike the case for compound semiconductors, carriers transferred across TMO interfaces occupy strongly correlated $3d$ bands. The limited kinetic hopping imposed by the interface combined with strong Coulomb interactions and Hund's coupling can lead to exchange interactions between transferred carriers. Such exchange interactions can lead to magnetism and to other forms of spin-ordered states.

Mechanisms that compensate for discontinuities in ionic polarization at interfaces are not limited to charge transfer. Structural degrees of freedom allow atomic-scale distortions, particularly distortions to the oxygen octahedra that surround transition metal ions, to arise in the lattice. Such distortions can affect the single-particle bandwidth because carrier hopping occurs between transition metal sites via oxygen ions. If sufficiently strong, such distortions to the oxygen octahedra can further lift degeneracies among $3d$ orbitals of transition metals, giving rise to orbital occupation that does not exist in bulk compounds (35, 36).

Much of the interest in correlated effects at TMO interfaces has emerged from the discovery of a quasi-two-dimensional electron gas at the interface between LaAlO_3 and SrTiO_3 (37, 38). Along the [100] direction, LaAlO_3 has alternating planes of LaO and AlO_2 that are nominally $+1$ and -1 in ionic charge, respectively. In contrast, the alternating planes of SrO and TiO_2 along the [001] direction of SrTiO_3 are charge neutral. Interfaces between LaAlO_3 and SrTiO_3 in the [001] direction thus exhibit a discontinuity in the polarization. The formation of a quasi-two-dimensional electron gas is believed to compensate for the discontinuity in polarization. Investigators have proposed several mechanisms to explain the origin of the carriers, such as charge transfer from LaAlO_3 to SrTiO_3 , oxygen vacancies in the SrTiO_3 , and intermixing of La and Sr cations (39, 40). The latter two extrinsic sources of carriers can be minimized or eliminated through careful control of growth conditions (41). The origin of intrinsic carriers transferred from the LaAlO_3 is still not clear. One model suggests that carriers are transferred from the valence band of LaAlO_3 to the conduction band of SrTiO_3 (42). However, recent synchrotron X-ray photoemission experiments found that the polar electric field in the LaAlO_3 is too small to allow charge transfer from the valence band to occur (43, 44). Instead, electron donors such as oxygen vacancies at the surface of LaAlO_3 are believed to provide the carriers to the interface to form the two-dimensional electron gas (45, 46).

Here we highlight two correlated phenomena at the $\text{LaAlO}_3/\text{SrTiO}_3$ interface, namely superconductivity and magnetism (47–52). The latter is particularly intriguing, given that SrTiO_3 and LaAlO_3 do not exhibit magnetism in the bulk. Yet even more unexpected is that superconductivity and magnetism have been found to coexist, because the two forms of quantum order are in general mutually exclusive. Evidence from transport and X-ray absorption spectroscopy measurements suggests that two types of carriers exist at $\text{LaAlO}_3/\text{SrTiO}_3$ heterojunctions: high-mobility carriers

situated away from the interface and low-mobility carriers prone to localization at the interface (43, 44, 53, 54). Magnetism (superconductivity) has been associated with the latter (former) type of carriers. Supporting the idea of localized carriers, density functional calculations indicate that the band structure at the $\text{LaAlO}_3/\text{SrTiO}_3$ interface has multiple subbands occupied by carriers with heavy and light masses, which exhibit low and high mobilities, respectively (55).

The magnetism that arises at the $\text{LaAlO}_3/\text{SrTiO}_3$ interface demonstrates that oxide interfaces can exhibit correlated phases that have not been observed in the bulk of either constituent. Thus, the search for correlated effects at TMO interfaces should not be limited to heterojunctions between oxides that exhibit correlated phases in the bulk. The $\text{LaAlO}_3/\text{SrTiO}_3$ interface also highlights the important role that discontinuities in polarization play in the emergence of correlated phases. The strong electric fields at interfaces between polar materials and nonpolar materials can produce band structures that support strong correlations for which there is no bulk analog. Conducting electron gases and strong correlations have also been found at interfaces between SrTiO_3 and other types of polar oxides, including LaTiO_3 (56), GdTiO_3 (57), LaVO_3 (58), and LaGaO_3 (59). The first three polar oxides are also Mott insulators, whereas the fourth is a conventional band insulator.

The conductivity and correlated effects found at the $\text{LaAlO}_3/\text{SrTiO}_3$ interface can be controlled through applied electric fields. For example, the electric field effect has been implemented to tune superconductivity at the $\text{LaAlO}_3/\text{SrTiO}_3$ interface by using the SrTiO_3 substrate as the gate dielectric (47). Due to the thicknesses of typical SrTiO_3 substrates, applied voltages of >100 V were required to effect appreciable changes in the density of carriers. Integrating thinner dielectrics reduced the magnitude of voltages required to modulate carrier density. For example, Förg et al. (60) fabricated $\text{LaAlO}_3/\text{SrTiO}_3$ -based field-effect transistors that showed current and voltage gain at room temperature by using the LaAlO_3 layer as a gate dielectric. For $\text{LaAlO}_3/\text{SrTiO}_3$ samples in which the LaAlO_3 layer is precisely three unit cells thick, the electron gas at the interface can be reversibly created and destroyed by applying voltages through a scanning probe tip. Cen et al. (61) used a scanning probe tip to laterally define nanoscale wires and devices on the surfaces of $\text{LaAlO}_3/\text{SrTiO}_3$ samples. The relative simplicity of using a scanning probe tip to create devices circumvents the challenges associated with creating nanoscale devices by using conventional lithography (61).

If properly understood, the electronic and structural degrees of freedom found at TMO interfaces provide a pathway to realize entirely new correlated materials. For example, recent interest has focused on creating nickelate-based heterostructures that are electronic analogs to the superconducting cuprates (62). For LaNiO_3 , the Ni ion is in a $3d^7$ configuration in which a single electron is shared between degenerate $d_{3z^2-r^2}$ and $d_{x^2-y^2}$ orbitals. In comparison, the Cu ion in cuprate superconductors is in a $3d^9$ configuration characterized by a singly occupied $3d_{x^2-y^2}$ orbital. The two-dimensional nature of the singly occupied $3d_{x^2-y^2}$ orbital combined with strong Coulomb repulsion gives rise to the antiferromagnetic state that is essential for superconductivity. Density functional calculations by Chen et al. (63) showed that the general principles of charge transfer and symmetry breaking at TMO interfaces can be applied to create a singly occupied $3d_{x^2-y^2}$ orbital in LaNiO_3 . Controlling orbital occupation in artificial TMO heterostructures would open a new paradigm in materials development and in the study of correlated phenomena.

BANDWIDTH CONTROL IN CORRELATED OXIDE HETEROSTRUCTURES

Control of the single-particle bandwidth provides another method by which to manipulate correlated behavior in TMOs. Recent studies have elucidated key relationships between structure and

transport in ultrathin films. Furthermore, device geometries designed to manipulate atomic-scale structure through applied electric fields are beginning to emerge. Integrating correlated TMOs into such device geometries could lead to active devices in which metal-insulator transitions and other correlated effects are manipulated through structural changes.

Carrier itinerancy in TMOs is determined largely by the degree to which transition metal $3d$ and oxygen $2p$ orbitals hybridize, because carriers hop between transition metal sites via oxygen ions. Wave functions for $3d$ orbitals are spatially more confined, and thus subtle changes in bond angles can have large effects on orbital overlap and hybridization. Interfaces and free surfaces break the translational symmetry of the lattice, leading to changes in the electrostatic boundary conditions that affect bonding and atomic-scale structure. As films approach λ_{el} in thickness, changes in atomic structure near interfaces and surfaces have an increasingly pronounced effect on transport properties and correlated behavior. For example, Disa et al. (64) found that the metal-insulator transition temperature in ultrathin $\text{Nd}_{1-y}\text{La}_y\text{NiO}_3$ films is renormalized to lower temperatures when such films are grown under compressive strain on LaAlO_3 substrates. X-ray diffraction measurements and soft-X-ray absorption spectroscopy confirmed that the renormalized transition temperature is due to the enhanced Ni-O bond hybridization associated with compressive strain.

The example of $\text{Nd}_{1-y}\text{La}_y\text{NiO}_3$ discussed above highlights static atomic distortions that affect carrier transport and correlated behavior. Structural distortions can also give rise to dynamic effects, i.e., phonons, that influence carrier scattering. For example, in ultrathin films of $\text{La}_{1-x}\text{Sr}_x\text{MnO}_3$ ($x=0.47$) grown on single-crystal SrTiO_3 substrates, a pronounced cusp in the resistivity appears as a function of temperature near 108 K (65). This cusp coincides with a structural transition that is characterized by rotation of the TiO_6 octahedra in SrTiO_3 to an antiferrodistortive configuration (66). Because the $\text{La}_{1-x}\text{Sr}_x\text{MnO}_3$ is coherently strained to the SrTiO_3 substrate, rotations in the TiO_6 octahedra propagate across the interface and cause the corresponding MnO_6 octahedra to also rotate in the first few unit cells. As this structural transition in SrTiO_3 is approached from both directions in temperature, there is a divergence in the occupation of phonon modes associated with the TiO_6 and MnO_6 octahedral rotations. These phonons are particularly effective at disturbing the hybridization between Mn $3d$ and O $2p$ orbitals, leading to the cusp observed in the resistivity.

Relationships between atomic-scale structure and electronic transport in TMOs could potentially be exploited to actively control transport behavior in devices. For example, the cusp in resistivity observed in $\text{La}_{1-x}\text{Sr}_x\text{MnO}_3$ films can be suppressed by electrostatically pulling carriers away from the $\text{La}_{1-x}\text{Sr}_x\text{MnO}_3/\text{SrTiO}_3$ interface, where phonon scattering is most intense. The electrostatic movement of carriers was achieved by switching the polarization of a ferroelectric gate grown on top of the $\text{La}_{1-x}\text{Sr}_x\text{MnO}_3$. Conversely, electrostatically pushing carriers toward the $\text{La}_{1-x}\text{Sr}_x\text{MnO}_3/\text{SrTiO}_3$ interface restored the cusp in resistivity (65).

More-ambitious device geometries aimed at inducing macroscopic structural changes to modify bandwidth are just beginning to be proposed. Newns et al. (67) recently proposed a so-called piezoelectronic transistor (PET) that uses a piezoelectric gate to mechanically compress a conducting channel composed of a piezoresistive material (**Figure 7**). Calculations indicate that the PET has the potential to be a high-speed, low-power switch that could replace CMOS-based devices, provided that highly piezoresistive channel materials can be found or developed. The high sensitivity to pressure is necessary to realize PETs that exhibit sufficiently high on-off ratios comparable to those of present CMOS devices. Oxides that exhibit metal-insulator transitions under applied pressure, such as $(\text{V}_{1-x}\text{Cr}_x)_2\text{O}_3$, are thus ideal candidate materials to be used in PETs (68). However, candidate channel materials are not limited to materials that exhibit piezoresistivity in the bulk. Given that ultrathin films of TMOs, such as LaNiO_3 , are prone to

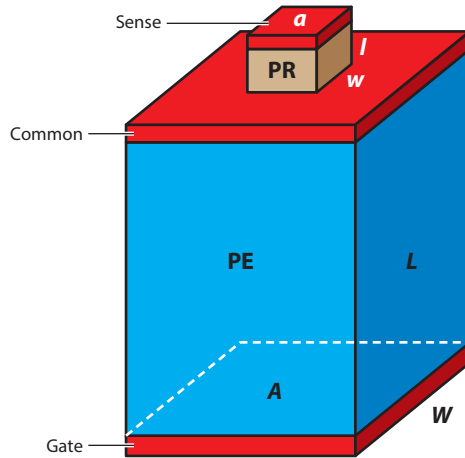


Figure 7

Schematic of a piezoelectronic transistor showing the piezoelectric (PE) and piezoresistive (PR) elements, along with metallic contacts (*red*). The PE layer applies strain to the PR layer, inducing changes in resistivity. Such device geometry could be utilized to actively induce macroscopic structural changes in a transition metal oxide with altered materials behavior or phase. Reproduced with permission from Reference 67.

atomic-scale distortions that affect bandwidth, actively inducing structural changes that give rise to piezoresistive effects may be possible.

FUTURE OUTLOOK

Beyond developing methods to control correlated phenomena in device geometries, elucidating materials behavior on nanometer length scales is also required. Recent studies have revealed that the electronic structure of a correlated TMO can be spatially inhomogeneous at nanometer length scales. For example, doped carriers can self-organize into stripes or checkerboard patterns in underdoped cuprates (69, 70). Also, the size of the superconducting gap varies spatially across the surfaces of cleaved crystals (71). The manganites provide another example of electronic inhomogeneity. The competition between ferromagnetic metallic phases and antiferromagnetic insulating phases gives rise to phase separation; e.g., a crystal divides into spatial clusters exhibiting dissimilar phases. Phase separation has been established to be essential for the phenomenon of CMR, in which large changes in resistivity can be driven by applied magnetic fields. Evidence for electronic inhomogeneity has been found in a variety of oxide systems (72), suggesting that inhomogeneity may be present in TMOs in which competition between phases is important. Quenched disorder in the form of, for example, dopant-induced lattice distortions and nonstatistical distributions of dopants apparently plays a key role in the emergence of electronic inhomogeneity.

Electronic inhomogeneity presents both opportunities and challenges in the development of correlated TMO-based devices. Candidate materials for post-CMOS technology will need to exhibit behavior that is consistently reproduced as materials dimensions are decreased to nanometer length scales. Thus, on the one hand, electronic inhomogeneity and quenched disorder are potential challenges in the development of scalable devices. Controlling sources of quenched disorder from materials synthesis will be key to mitigating such issues. On the other hand, electronic inhomogeneity in TMOs also opens a potential pathway to realize materials that exhibit unusual

nonlinear effects such as CMR (73). For CMR, the phase-separated state that characterizes manganites is composed of ferromagnetic metallic and antiferromagnetic insulating clusters. Application of a field aligns the randomly oriented moments of ferromagnetic clusters, leading to enhanced carrier hopping between such clusters. Experiments have demonstrated that the disorder-induced phase-separated clusters in the manganites are essential for CMR (74). In principle, materials that exhibit a giant or colossal response to other types of perturbations such as electric fields, temperature, and pressure could potentially be realized by controlling phase separation in TMOs (73). Materials that exhibit a giant or colossal response to perturbation would be particularly useful in microelectronic and sensing devices.

Finally, materials behavior may not follow the bulk phase diagram as sample dimensions are reduced to nanometer length scales. Finite size effects can enhance or suppress various types of quantum order, leading to unusual effects in materials behavior. For example, fluctuations in the transport characteristics of nanowires made from underdoped $\text{YBa}_2\text{Cu}_3\text{O}_{7-\delta}$ have been observed (75). These fluctuations have been attributed to fluctuating domain structures possibly associated with the stripe order found in underdoped cuprates (69). Such effects are anticipated to emerge in materials in which several phases may coexist and compete (76). Thus, elucidating how correlated behavior evolves as materials dimensions are reduced is also essential for the development of TMO-based electronic devices.

CONCLUSION

With the advancements in materials growth, characterization, and device fabrication discussed above, the outlook for electronic devices based on correlated TMOs is promising. Progress in materials growth has made the fabrication of high-quality conducting channels that are comparable to λ_{el} in thickness a reality. Furthermore, the use of alternative gate materials, such as ionic electrolytes, has enabled changes to areal carrier density of up to $\sim 10^{15} \text{ cm}^{-2}$ possible. Such advancements have enabled magnetism, superconductivity, and metal-insulator transitions to be controlled through the electric field effect. Interfaces between TMOs have emerged as a setting in which correlated behavior can be manipulated in quasi-two dimensions to realize quantum-ordered phases that do not exist in bulk oxides. Moreover, the reduced dimensionality of interfaces is particularly amenable to integration into field-effect devices. Finally, key relationships between structure and transport in ultrathin films of TMOs have been elucidated. Integrating TMOs into novel device geometries could allow applied electric fields to control bandwidth by coupling to structural degrees of freedom. Bandwidth control of transport and correlated behavior in TMOs could open the pathway to a new generation of devices that use less power than is presently possible. Thus, TMO-based heterostructures and devices promise to reveal fundamental physics and to be a source of useful technology in the years to come.

DISCLOSURE STATEMENT

The authors are not aware of any affiliations, memberships, funding, or financial holdings that might be perceived as affecting the objectivity of this review.

ACKNOWLEDGMENTS

The authors acknowledge support from NSF MRSEC DMR-1119826 (CRISP), NSF DMR-1309868, ONR, AFOSR, and FAME.

LITERATURE CITED

1. News DM, Misewich JA, Tsuei CC, Gupta A, Scott BA, Schrott A. 1998. Mott transition field effect transistor. *Appl. Phys. Lett.* 73:780–82
2. McKee RA, Walker FJ, Chisholm MF. 1998. Crystalline oxides on silicon: the first five monolayers. *Phys. Rev. Lett.* 81:3014–17
3. Kumah DP, Reiner JW, Segal Y, Kolpak AM, Zhang Z, et al. 2010. The atomic structure and polarization of strained SrTiO₃/Si. *Appl. Phys. Lett.* 97:251902
4. ITRS. 2011. Emerging research materials. In *International Technology Roadmap for Semiconductors*, Chapter 11. <http://www.itrs.net/Links/2011ITRS/2011Chapters/2011ERD.pdf>
5. Zaanen J, Sawatzky GA, Allen JW. 1985. Band gaps and electronic structure of transition-metal compounds. *Phys. Rev. Lett.* 55:418–21
6. Imada M, Fujimori A, Tokura Y. 1998. Metal-insulator transitions. *Rev. Mod. Phys.* 70:1039–263
7. Ahn C, Triscone J, Mannhart J. 2003. Electric field effect in correlated oxide systems. *Nature* 424:1015–18
8. Hong X, Posadas A, Ahn CH. 2005. Examining the screening limit of field effect devices via the metal-insulator transition. *Appl. Phys. Lett.* 86:142501
9. Vaz CAF, Hoffman J, Ahn CH, Ramesh R. 2010. Magnetoelectric coupling effects in multiferroic complex oxide composite structures. *Adv. Mater.* 22:2900–18
10. Molegraaf HJA, Hoffman J, Vaz CAF, Gariglio S, van der Marel D, et al. 2009. Magnetoelectric effects in complex oxides with competing ground states. *Adv. Mater.* 21:3470–74
11. Vaz CAF, Hoffman J, Segal Y, Reiner JW, Grober RD, et al. 2010. Origin of the magnetoelectric coupling effect in Pb(Zr_{0.2}Ti_{0.8})O₃/La_{0.8}Sr_{0.2}MnO₃ multiferroic heterostructures. *Phys. Rev. Lett.* 104:127202
12. Mannhart J. 1996. High-T_c transistors. *Supercond. Sci. Technol.* 9:49–67
13. Ahn CH, Gariglio S, Paruch P, Tybell T, Antognazza L, Triscone J-M. 1999. Electrostatic modulation of superconductivity in ultrathin GdBa₂Cu₃O_{7-x} films. *Science* 284:1152–55
14. Ueno K, Nakamura S, Shimotani H, Ohtomo A, Kimura N, et al. 2008. Electric-field-induced superconductivity in an insulator. *Nat. Mater.* 7:855–58
15. Ye JT, Inoue S, Kobayashi K, Kasahara Y, Yuan HT, et al. 2010. Liquid-gated interface superconductivity on an atomically flat film. *Nat. Mater.* 9:125–28
16. Bollinger AT, Dubuis G, Yoon J, Pavuna D, Misewich J, Bozovic I. 2011. Superconductor-insulator transition in La_{1-x}Sr_xCuO₄ at the pair quantum resistance. *Nature* 472:458–60
17. Emery VJ, Kivelson SA. 1995. Importance of phase fluctuations in superconductors with small superfluid density. *Nature* 374:434–37
18. Lee PA, Nagaosa N, Wen X-G. 2006. Doping a Mott insulator: physics of high-temperature superconductivity. *Rev. Mod. Phys.* 78:17–85
19. Timusk T, Statt B. 1999. The pseudogap in high-temperature superconductors: an experimental survey. *Rep. Prog. Phys.* 62:61–122
20. Yang H, Yang S-H, Takahashi S, Parkin SSP. 2010. Extremely long quasiparticle spin lifetimes in superconducting aluminium using MgO tunnel spin injectors. *Nat. Mater.* 9:586–93
21. Vas'ko VA, Larkin VA, Kraus PA, Nikolaev KR, Grupp DE, et al. 1997. Critical current suppression in a superconductor by injection of spin-polarized carriers from a ferromagnet. *Phys. Rev. Lett.* 78:1134–37
22. Ngai J, Tseng YC, Morales P, Pribiag V, Wei JYT, et al. 2004. Scanning tunneling spectroscopy under pulsed spin injection. *Appl. Phys. Lett.* 84:1907–9
23. Fu C-C, Huang Z, Yeh N-C. 2002. Spin-polarized quasiparticle transport in cuprate superconductors. *Phys. Rev. B* 65:224516
24. Dong ZW, Ramesh R, Venkatesan T, Johnson M, Chen ZY, et al. 1997. Spin-polarized quasiparticle injection devices using Au/YBa₂Cu₃O₇/LaAlO₃/Nd_{0.7}Sr_{0.3}MnO₃ heterostructures. *Appl. Phys. Lett.* 71:1718–20
25. Stroud RM, Kim J, Eddy CR, Chrisey DB, Horwitz JS, et al. 1998. Fabrication of YBa₂Cu₃O₇/SrTiO₃/La_{0.7}Sr_{0.3}MnO₃ junctions for the control of supercurrent by spin-polarized quasiparticle current injection. *J. Appl. Phys.* 83:7189–91
26. Scherwitzl R, Zubko P, Lezama IG, Ono S, Morpurgo AF, et al. 2010. Electric-field control of the metal-insulator transition in ultrathin NdNiO₃ films. *Adv. Mater.* 22:5517–20

27. Ha SD, Vetter U, Shi J, Ramanathan S. 2013. Electrostatic gating of metallic and insulating phases in SmNiO_3 . *Appl. Phys. Lett.* 102:183102
28. Son J, Jalan B, Kajdos A, Balents L, Allen SJ, Stemmer S. 2011. Probing the metal-insulator transition in NdNiO_3 by electrostatic doping. *Appl. Phys. Lett.* 99:192107
29. Nakano M, Shibuya K, Okuyama D, Hatano T, Ono S, et al. 2012. Collective bulk carrier delocalization driven by electrostatic surface charge accumulation. *Nature* 487:459–62
30. Jeong J, Aetukuri N, Graf T, Schladt TD, Samant MG, Parkin SSP. 2013. Suppression of metal-insulator transition in VO_2 by electric field-induced oxygen vacancy formation. *Science* 339:1402–5
31. Rabe K, Ahn C, Triscone J-M, eds. 2007. *Physics of Ferroelectrics: A Modern Perspective*. Berlin: Springer-Verlag
32. Hwang HY, Iwasa Y, Kawasaki M, Keimer B, Nagaosa N, Tokura Y. 2012. Emergent phenomena at oxide interfaces. *Nat. Mater.* 11:103–13
33. Dingle R, Stormer HL, Gossard AC, Wiegmann W. 1978. Electron mobilities in modulation-doped semiconductor heterojunction superlattices. *Appl. Phys. Lett.* 33:665–67
34. Ambacher O, Smart J, Shealy JR, Weimann NG, Chu K, et al. 1999. Two-dimensional electron gases induced by spontaneous and piezoelectric polarization charges in N- and Ga-face AlGaIn/GaN heterostructures. *J. Appl. Phys.* 85:3222–33
35. Chakhalian J, Freeland JW, Habermeier H-U, Cristiani G, Khaliullin G, et al. 2007. Orbital reconstruction and covalent bonding at an oxide interface. *Science* 318:1114–17
36. Salluzzo M, Cezar JC, Brookes MB, Bisogni V, De Luca GM, et al. 2009. Orbital reconstruction and the two-dimensional electron gas at the $\text{LaAlO}_3/\text{SrTiO}_3$ interface. *Phys. Rev. Lett.* 102:166804
37. Ohtomo A, Hwang HY. 2004. A high-mobility electron gas at the $\text{LaAlO}_3/\text{SrTiO}_3$ heterointerface. *Nature* 427:423–26
38. Thiel S, Hammerl G, Schmehl A, Schneider CW, Mannhart J. 2006. Tunable quasi-two-dimensional electron gases in oxide heterostructures. *Science* 313:1942–45
39. Nakagawa N, Hwang HY, Muller DA. 2006. Why some interfaces cannot be sharp. *Nat. Mater.* 5:204–9
40. Herranz G, Basletic M, Bibes M, Carrertero C, Tafrá E, et al. 2007. High mobility in $\text{LaAlO}_3/\text{SrTiO}_3$ heterostructures: origin, dimensionality, and perspectives. *Phys. Rev. Lett.* 98:216803
41. Cantoni C, Gazquez J, Granozio FM, Oxley MP, Varela M, et al. 2012. Electron transfer and ionic displacements as the origin of the 2D electron gas at the LAO/STO interface: direct measurements with atomic-column spatial resolution. *Adv. Mater.* 24:3952–57
42. Chen H, Kolpak A, Ismail-Beigi S. 2010. Electronic and magnetic properties of $\text{SrTiO}_3/\text{LaAlO}_3$ interfaces from first principles. *Adv. Mater.* 22:2881–99
43. Takizawa M, Tsuda S, Susaki T, Hwang HY, Fujimori A. 2011. Electronic charges and electric potential at $\text{LaAlO}_3/\text{SrTiO}_3$ interfaces studied by core-level photoemission spectroscopy. *Phys. Rev. B* 84:245124
44. Slooten E, Zhong Z, Molegraaf HJA, Eerkes PD, de Jong S, et al. 2013. Hard X-ray photoemission and density functional theory study of the internal electric field in $\text{SrTiO}_3/\text{LaAlO}_3$ oxide heterostructures. *Phys. Rev. B* 87:085128
45. Bristowe NC, Littlewood PB, Artacho E. 2011. Surface defects and conduction in polar oxide heterostructures. *Phys. Rev. B* 83:205405
46. Bi F, Bogorin DF, Cen C, Bark CW, Park J-W, et al. 2010. “Water-cycle” mechanism for writing and erasing nanostructures at the $\text{LaAlO}_3/\text{SrTiO}_3$ interface. *Appl. Phys. Lett.* 97:173110
47. Caviglia AD, Gariglio S, Reyren N, Jaccard D, Schneider T, et al. 2008. Electric field control of the $\text{LaAlO}_3/\text{SrTiO}_3$ interface ground state. *Nature* 456:624–27
48. Brinkman A, Huijben M, van Zalk M, Huijben J, Zeitler U, et al. 2007. Magnetic effects at the interface between non-magnetic oxides. *Nat. Mater.* 6:493–96
49. Bert JA, Kalisky B, Bell C, Kim M, Hikita Y, et al. 2011. Direct imaging of the coexistence of ferromagnetism and superconductivity at the $\text{LaAlO}_3/\text{SrTiO}_3$ interface. *Nat. Phys.* 7:767–71
50. Dikin DA, Mehta M, Bark CW, Folkman CM, Eom C-B, Chandrasekhar V. 2011. Coexistence of superconductivity and ferromagnetism in two dimensions. *Phys. Rev. Lett.* 107:056802
51. Li L, Richter C, Mannhart J, Ashoori RC. 2011. Coexistence of magnetic order and two-dimensional superconductivity at $\text{LaAlO}_3/\text{SrTiO}_3$ interfaces. *Nat. Phys.* 7:762–66

52. Ariando, Wang X, Baskaran G, Liu ZQ, Huijben J, et al. 2011. Electronic phase separation at the $\text{LaAlO}_3/\text{SrTiO}_3$ interface. *Nat. Commun.* 2:188
53. Sing M, Berner G, Goß K, Müller A, Ruff A, et al. 2009. Profiling the interface electron gas of $\text{LaAlO}_3/\text{SrTiO}_3$ heterostructures with hard X-ray photoelectron spectroscopy. *Phys. Rev. Lett.* 102:176805
54. Seo SSA, Marton Z, Choi WS, Hassink GWJ, Blank DHA, et al. 2009. Multiple conducting carriers generated in $\text{LaAlO}_3/\text{SrTiO}_3$ heterostructures. *Appl. Phys. Lett.* 95:082107
55. Popovic ZS, Satpathy S, Martin RM. 2008. Origin of the two-dimensional electron gas carrier density at the LaAlO_3 on SrTiO_3 interface. *Phys. Rev. Lett.* 101:256801
56. Biscaras J, Bergeal N, Kushwaha A, Wolf T, Rastogi A, et al. 2010. Two-dimensional superconductivity at a Mott insulator/band insulator interface $\text{LaAlO}_3/\text{SrTiO}_3$. *Nat. Commun.* 1:89
57. Moetakef P, Zhang JY, Kozhanov A, Jalan B, Seshadri R, et al. 2011. Transport in ferromagnetic $\text{GdTiO}_3/\text{SrTiO}_3$ heterostructures. *Appl. Phys. Lett.* 98:112110
58. Hotta Y, Susaki T, Hwang HY. 2007. Polar discontinuity doping of the $\text{LaVO}_3/\text{SrTiO}_3$ interface. *Phys. Rev. Lett.* 99:236805
59. Perna P, Maccariello D, Radovic M, Scotti di Uccio U, Pallecchi I, et al. 2010. Conducting interfaces between band insulating oxides: the $\text{LaGaO}_3/\text{SrTiO}_3$ heterostructure. *Appl. Phys. Lett.* 97:152111
60. Förg B, Richter C, Mannhart J. 2012. Field-effect devices utilizing LaAlO_3 - SrTiO_3 interfaces. *Appl. Phys. Lett.* 100:053506
61. Cen C, Thiel S, Mannhart J, Levy J. 2009. Oxide nanoelectronics on demand. *Science* 323:1026–30
62. Hansmann P, Yang X, Toschi A, Khaliullin G, Andersen OK, Held K. 2009. Turning a nickelate Fermi surface into a cupratelike one through heterostructuring. *Phys. Rev. Lett.* 103:016401
63. Chen H, Kumah DP, Disa AS, Walker FJ, Ahn CH, Ismail-Beigi S. 2013. Modifying the electronic orbitals of nickelate heterostructures via structural distortions. *Phys. Rev. Lett.* 110:186402
64. Disa AS, Kumah DP, Ngai JH, Specht ED, Arena DA, et al. 2013. Phase diagram of compressively strained nickelate thin films. *APL Mater.* 1:032110
65. Segal Y, Garrity KF, Vaz CAF, Hoffman JD, Walker FJ, et al. 2011. Dynamic evanescent phonon coupling across the $\text{La}_{1-x}\text{Sr}_x\text{MnO}_3/\text{SrTiO}_3$ interface. *Phys. Rev. Lett.* 107:105501
66. Scott J. 1974. Soft-mode spectroscopy: experimental studies of structural phase transitions. *Rev. Mod. Phys.* 46:83–128
67. Newns D, Elmegreen B, Liu XH, Martyna G. 2012. High response piezoelectric and piezoresistive materials for fast, low voltage switching: simulation and theory of transduction physics at the nanometer-scale. *Adv. Mater.* 24:3672–77
68. McWhan DB, Reimeika JP. 1970. Metal-insulator transition in $(\text{V}_{1-x}\text{Cr}_x)_2\text{O}_3$. *Phys. Rev. B* 2:3734–50
69. Tranquada JM, Sternlieb BJ, Axe JD, Nakamura Y, Uchida S. 1995. Evidence for stripe correlations of spins and holes in copper oxide superconductors. *Nature* 375:561–63
70. Hanaguri T, Lupien C, Kohsaka Y, Lee D-H, Azuma M, et al. 2004. A “checkerboard” electronic crystal state in lightly hole-doped $\text{Ca}_{2-x}\text{Na}_x\text{CuO}_2\text{Cl}_2$. *Nature* 430:1001–5
71. Lang KM, Madhavan V, Hoffman JE, Hudson EW, Eisaki H, et al. 2002. Imaging the granular structure of high- T_C superconductivity in underdoped $\text{Bi}_2\text{Sr}_2\text{CaCu}_2\text{O}_{8+\delta}$. *Science* 415:412–16
72. Qazilbash MM, Brehm M, Chae BG, Ho P-C, Andreev GO, et al. 2007. Mott transition in VO_2 revealed by infrared spectroscopy and nano-imaging. *Science* 318:1750–53
73. Dagatto E. 2005. Complexity in strongly correlated electronic systems. *Science* 309:257–62
74. Akahoshi D, Uchida M, Tomioka Y, Arima T, Matsui Y, Tokura Y. 2003. Random potential effect near the bicritical region in perovskite manganites as revealed by comparison with the ordered perovskite analogs. *Phys. Rev. Lett.* 90:177203
75. Bonetti JA, Caplan DS, Van Harlingen DJ, Weissman MB. 2004. Electronic transport in underdoped $\text{YBa}_2\text{Cu}_3\text{O}_{7-\delta}$ nanowires: evidence for fluctuating domain structures. *Phys. Rev. Lett.* 93:087002
76. Ghiringhelli G, Le Tacon M, Minola M, Blanco-Canosa S, Mazzoli C, et al. 2012. Long-range incommensurate charge fluctuations in $(\text{Y,Nd})\text{Ba}_2\text{Cu}_3\text{O}_{6+x}$. *Science* 337:821–25